

# A nonlinear calcification response to CO<sub>2</sub>-induced ocean acidification by the coral *Oculina arbuscula*

J. B. Ries · A. L. Cohen · D. C. McCorkle

Received: 15 August 2009 / Accepted: 28 April 2010  
© Springer-Verlag 2010

**Abstract** Anthropogenic elevation of atmospheric  $p\text{CO}_2$  is predicted to cause the pH of surface seawater to decline by 0.3–0.4 units by 2100 AD, causing a 50% reduction in seawater  $[\text{CO}_3^{2-}]$  and undersaturation with respect to aragonite in high-latitude surface waters. We investigated the impact of CO<sub>2</sub>-induced ocean acidification on the temperate scleractinian coral *Oculina arbuscula* by rearing colonies for 60 days in experimental seawaters bubbled with air-CO<sub>2</sub> gas mixtures of 409, 606, 903, and 2,856 ppm  $p\text{CO}_2$ , yielding average aragonite saturation states ( $\Omega_A$ ) of 2.6, 2.3, 1.6, and 0.8. Measurement of calcification (via buoyant weighing) and linear extension (relative to a <sup>137</sup>Ba/<sup>138</sup>Ba spike) revealed that skeletal accretion was only minimally impaired by reductions in  $\Omega_A$  from 2.6 to 1.6, although major reductions were observed at 0.8 (undersaturation). Notably, the corals continued accreting new skeletal material even in undersaturated conditions, although at reduced rates. Correlation between rates of linear extension and calcification suggests that reduced calcification under  $\Omega_A = 0.8$  resulted from reduced aragonite accretion, rather than from localized dissolution. Accretion of pure aragonite under each  $\Omega_A$  discounts the possibility that these corals will begin producing calcite, a less soluble form of CaCO<sub>3</sub>, as the oceans acidify. The corals' nonlinear response to reduced  $\Omega_A$  and their ability to accrete

new skeletal material in undersaturated conditions suggest that they strongly control the biomineralization process. However, our data suggest that a threshold seawater  $[\text{CO}_3^{2-}]$  exists, below which calcification within this species (and possibly others) becomes impaired. Indeed, the strong negative response of *O. arbuscula* to  $\Omega_A = 0.8$  indicates that their response to future  $p\text{CO}_2$ -induced ocean acidification could be both abrupt and severe once the critical  $\Omega_A$  is reached.

**Keywords** Ocean acidification · Temperate corals · Calcification · Aragonite saturation state · Carbon dioxide (CO<sub>2</sub>) · pH

## Introduction

Atmospheric  $p\text{CO}_2$  has increased from ~280 to nearly 400 ppm since the Industrial Revolution in the late 1700s (Keeling 1960; Neftel et al. 1985; Rahmstorf et al. 2007; Keeling et al. 2009), largely because of the anthropogenic combustion of fossil fuels and deforestation. This rate of increase is at least 10 times greater than what is thought to have occurred over the past several million years (Doney and Schimel 2007), resulting in a current partial pressure that represents the highest level in at least the past 800,000 years (Luthi et al. 2008). This largely anthropogenic increase in atmospheric  $p\text{CO}_2$  has caused the pH of surface seawater to decrease by ~0.1 units since the Industrial Revolution (Raven et al. 2005). If atmospheric  $p\text{CO}_2$  reaches the 700–900 ppm range that is predicted by the Intergovernmental Panel on Climate Change (scenarios A1B, IS92A, A2, A1F1; Houghton et al. 2001) for the end of the 21st century, then the pH of high-latitude surface seawater will decrease by another 0.3–0.4 units (Brewer 1997), resulting in a nearly 50% reduction in the carbonate

Communicated by Environment Editor Prof. Rob van Woesik

J. B. Ries (✉) · A. L. Cohen · D. C. McCorkle  
Department of Geology and Geophysics, Woods Hole  
Oceanographic Institution, Woods Hole, MA 02543, USA  
e-mail: jries@unc.edu

J. B. Ries  
Department of Marine Sciences, University of North Carolina,  
Chapel Hill, 333 Chapman Hall, Campus Box 3300, Chapel Hill,  
NC 27599, USA

ion concentration [ $\text{CO}_3^{2-}$ ] of seawater. This decrease in [ $\text{CO}_3^{2-}$ ] will reduce the saturation state of seawater with respect to the calcium carbonate ( $\text{CaCO}_3$ ) minerals aragonite and calcite, the material that many marine organisms use to build their shells and skeletons.

Multiple experimental studies have shown that the calcification rates of a wide range of marine organisms decline when they are reared in experimental seawaters having the carbonate chemistry and/or pH values predicted to occur over the coming centuries due to  $\text{CO}_2$ -induced ocean acidification (for reviews, see Langdon 2000; Kleypas et al. 2006; Hoegh-Guldberg et al. 2007; Fabry et al. 2008; Doney et al. 2009). Many experiments on scleractinian (stony) corals reveal that skeletal growth generally declines relatively linearly with reductions in seawater [ $\text{CO}_3^{2-}$ ] (Marubini and Atkinson 1999; Marubini et al. 2001, 2003, 2008; Langdon and Atkinson 2005; Schneider and Erez 2006). However, recent experimental studies have shown that some tropical (Reynaud et al. 2003; Cohen et al. 2009; Jury et al. 2009) as well as temperate species (Rodolfo-Metalpa et al. 2010; Holcomb et al. 2010) of scleractinian corals exhibit either no response and/or a nonlinear response to  $\text{CO}_2$ -induced reductions in seawater [ $\text{CO}_3^{2-}$ ].

Here, we present the results of an experimental study designed to investigate the effects of  $\text{CO}_2$ -induced ocean acidification on the calcification (Ries et al. 2009), linear extension, and  $\text{CaCO}_3$  polymorph mineralogy of the temperate, zooxanthellate scleractinian coral *Oculina arbuscula*. Although this coral does not build coral reefs, it is widespread along the mid-Atlantic and southeastern coasts of the United States and constitutes an important component of benthic hardground shelf ecosystems (<200 m) within these regions (Ruppert and Fox 1988). *O. arbuscula* is recognized as a relatively adaptable species and is known to tolerate broad ranges of temperature (4–30°C), salinity (25–37), and light (Miller 1995; Piniak 2002). Seasonal temperature changes also expose the coral to large fluctuations in the saturation state of seawater with respect to its skeletal aragonite, resulting in near undersaturated conditions during the coldest times of the year ( $\Omega_A = 1.3$ ,  $p\text{CO}_2 = 400$  ppm, alkalinity = 2,100  $\mu\text{M}$ , salinity = 32,  $T = 4^\circ\text{C}$ ). The fact that *O. arbuscula* is exposed to near undersaturated conditions on a seasonal basis makes it a particularly intriguing organism to investigate in the context of  $\text{CO}_2$ -induced ocean acidification.

## Materials and methods

### Specimen collection

Nineteen zooxanthellate colonies of the *O. arbuscula* were collected offshore of Bogue Banks in the Outer Banks

region of North Carolina in August 2007 pursuant to local, state, and federal regulations. Immediately after collection, organisms were transported by airplane and automobile to the Marine Calcification Laboratory at the Woods Hole Oceanographic Institution, where they were placed in holding tanks bubbled with compressed ambient air ( $\sim 409$  ppm). After  $\sim 14$  days of acclimation to the laboratory conditions, 4 3-cm-long fragments were harvested from each of the 19 colonies. Fragments were mounted on rectangular acrylic slides with cyanoacrylate. One mounted specimen from each of the 19 coral colonies was transferred to each of the experimental seawaters (19 specimens per aquarium, 76 specimens in total) for an additional 14 days of acclimation prior to the start of the experiment.

### Experimental growth conditions

Comparably sized specimens of *O. arbuscula* were reared for 60 days (10 September–9 November 2007) in each of 4 38-liter glass aquaria (76 specimens in total) filled with 0.2  $\mu\text{m}$ -filtered seawater obtained from Great Harbor in Vineyard Sound off the coast of Cape Cod, Massachusetts. The experimental seawaters were continuously bubbled with air- $\text{CO}_2$  gas mixtures of 409, 606, 903, and 2,856 ppm  $p\text{CO}_2$ . The average initial buoyant weights ( $\pm$ standard error) of the specimens reared in the four seawater treatments [ $2,173 \pm 203$  mg,  $2,176 \pm 203$  mg,  $1,904 \pm 203$  mg,  $1,965 \pm 203$  mg; Table 3] did not significantly ( $P < 0.05$ ) differ from one another.

The experimental seawaters were maintained at  $25 \pm 1^\circ\text{C}$  using 50-Watt electric heaters. Each tank was continuously filtered with polyester fleece and activated carbon at the rate of 600 l/h. The aquaria were illuminated with 10 h/day of 426 Watts per square meter ( $\text{W}/\text{m}^2$ ) irradiance (T8, 8,000 K aquarium spectrum lamps). Each aquarium and attached filtration system was covered with plastic wrap to facilitate equilibration between the gas mixtures and the experimental seawaters and to minimize evaporative water-loss. Seventy-five percent seawater changes were made every 14 days using seawater bubbled with the appropriate air- $\text{CO}_2$  mixtures. Each coral fragment was fed 330 mg wet weight of previously frozen *Artemia* sp. every other day. The *Artemia* sp. were supplied to each of the corals' polyps as equitably as possible using a 1-ml graduated transfer pipette.

### Carbonate system manipulation and constraint

The experimental air- $\text{CO}_2$  gases were formulated ( $\pm$ SD) at 409 ( $\pm 6$ ), 606 ( $\pm 7$ ), 903 ( $\pm 12$ ), and 2,856 ( $\pm 54$ ) ppm  $p\text{CO}_2$  using Aalborg mass flow controllers, yielding average seawater saturation states ( $\pm$ SD) of 2.6 ( $\pm 0.26$ ), 2.3 ( $\pm 0.18$ ), 1.6 ( $\pm 0.18$ ), and 0.8 ( $\pm 0.07$ ) with respect to

**Table 1** Average measured  $p\text{CO}_2$  of the mixed gases [ $p\text{CO}_2$  (gas-m)], salinity (Sal), temperature (Temp), total alkalinity (Alk), and pH; average calculated dissolved inorganic carbon (DIC), carbonate ion concentration ( $[\text{CO}_3^{2-}]$ ), bicarbonate ion concentration ( $[\text{HCO}_3^-]$ ), dissolved  $\text{CO}_2$  ( $[\text{CO}_2]_{\text{(SW)}}$ ), aragonite saturation state ( $\Omega_{\text{A}}$ ), and  $p\text{CO}_2$  of the mixed gases in equilibrium with the experimental seawaters [ $p\text{CO}_2$  (gas-e)]. “SD” is standard deviation; “n” is sample size

Measured parameters				
$p\text{CO}_2$ (gas-m)				
(ppm-v)	409	606	903	2,856
SD	6	7	12	54
Range	401–415	596–616	886–919	2,802–2,936
n	10	10	10	10
Sal				
(psu)	31.7	31.6	31.7	31.5
SD	0.2	0.4	0.4	0.6
Range	31.5–31.9	31.1–31.9	31.1–32.1	30.6–32.0
n	10	10	10	10
Temp				
°C	25.0	24.9	24.9	25.2
SD	0.2	0.1	0.1	0.1
Range	24.7–25.1	24.7–25.0	24.8–25.1	25.1–25.2
n	10	10	10	10
Alk				
( $\mu\text{M}$ )	1,960	2,012	2,027	2,071
SD	30	37	30	48
Range	1,923–1,991	1,959–2,043	1,986–2,055	2,032–2,138
n	5	5	5	5
pH				
	8.11	8.03	7.85	7.48
SD	0.06	0.04	0.05	0.03
Range	8.03–8.18	7.99–8.08	7.82–7.93	7.45–7.52
n	10	10	10	10
Calculated parameters				
DIC				
( $\mu\text{M}$ )	1,738	1,824	1,907	2,070
SD	47	32	30	40
Range	1,699–1,802	1,778–1,851	1,876–1,946	2,040–2,126
n	5	5	5	5
$[\text{CO}_3^{2-}]$				
( $\mu\text{M}$ )	160	141	102	47
SD	16	11	11	4
Range	141–180	134–156	94–118	43–53
n	5	5	5	5
$[\text{HCO}_3^-]$				
( $\mu\text{M}$ )	1,565	1,667	1,780	1,957
SD	58	30	32	40
Range	1,509–1,645	1,628–1,699	1,756–1,823	1,927–2,011
n	5	5	5	5
$[\text{CO}_2]_{\text{(SW)}}$				
( $\mu\text{M}$ )	12.6	16.1	25.6	66.1
SD	2.3	1.4	3.1	3.5
Range	10.2–15.6	14.2–17.6	21.2–28.4	61.7–70.2
n	5	5	5	5

**Table 1** continued

$\Omega_{\text{A}}$	2.60	2.28	1.64	0.77
SD	0.26	0.18	0.18	0.07
Range	2.29–2.91	2.16–2.53	1.51–1.91	0.70–0.86
n	5	5	5	5
$p\text{CO}_2$ (gas-e)				
(ppm-v)	450	573	915	2,377
SD	83	52	110	128
Range	363–561	504–629	759–1,015	2,211–2,523
n	5	5	5	5

aragonite, the form of  $\text{CaCO}_3$  produced by scleractinian corals (Table 1). The three lowest  $p\text{CO}_2$  levels were employed to span the range of atmospheric  $p\text{CO}_2$  values that are predicted to occur on Earth over the next three centuries (Houghton et al. 2001), while the highest value was selected to investigate how corals might respond to conditions that were undersaturated with respect to their skeletal mineral aragonite. In addition, the highest  $p\text{CO}_2$  value was selected to mimic atmospheric  $p\text{CO}_2$  conditions that are thought to have occurred in Cretaceous time (Royer et al. 2004; Tyrrell and Zeebe 2004), an interval over which scleractinian corals temporarily relinquished their role as primary reef builders to the bimineralic (aragonite and calcite) rudist bivalves (Scott 1995).

The air- $\text{CO}_2$  gas mixtures were introduced to the aquaria with 6-inch microporous airstones secured to the base of the aquaria at  $\sim 30$  cm depth. Salinity, temperature, and pH of the experimental seawaters, and  $p\text{CO}_2$  of the mixed gases, were measured weekly, and total alkalinity was measured every 2 weeks (Table 1). Dissolved inorganic carbon (DIC),  $[\text{CO}_3^{2-}]$ , bicarbonate ion concentration ( $[\text{HCO}_3^-]$ ), dissolved  $\text{CO}_2$  ( $[\text{CO}_2]_{\text{(SW)}}$ ),  $\Omega_{\text{A}}$ , and  $p\text{CO}_2$  of the mixed gases in equilibrium with the experimental seawaters [ $p\text{CO}_2$  (gas-e)] were calculated from these measured parameters (Table 1).

#### Measured parameters (Table 1)

Mixed gas  $p\text{CO}_2$  was measured with a *Qubit S151* infrared  $p\text{CO}_2$  analyzer calibrated with certified air- $\text{CO}_2$  gas standards and commercial air- $\text{CO}_2$  gas mixtures (calibrated using certified air- $\text{CO}_2$  gas standards; precision =  $\pm 2.0\%$ ; accuracy =  $\pm 1.8\%$ ). Temperature was measured with a partial-immersion mercury-glass thermometer (precision =  $\pm 0.3\%$ , accuracy =  $\pm 0.4\%$ ). Salinity was determined using an *Autosal* conductivity meter in the WHOI Hydrographic Laboratory and/or using a refractometer calibrated with simultaneous measurements of conductivity (precision =  $\pm 0.3\%$ ; accuracy =  $\pm 0.4\%$ ). Total alkalinity of seawater in each aquarium was determined via small

(precision =  $\pm 0.5\%$ , accuracy =  $\pm 0.5\%$ ) and/or large volume Gran titrations (precision =  $\pm 0.3\%$ , accuracy =  $\pm 0.3\%$ ) calibrated with certified Dickson alkalinity/DIC standards. Alkalinity determinations were made every 14 days at the midpoint between water changes. The authors acknowledge that this approach may underestimate the variance in alkalinity resulting from drawdown of  $\text{CO}_3^{2-}$  via calcification. Nevertheless, because the alkalinity determinations were made at the 7-day midpoint between water changes, the measured alkalinity should represent the approximate average value for the experimental seawaters across the 14-day interval between water changes. Seawater pH (precision =  $\pm 0.005$ ; accuracy =  $\pm 0.02$ ) was determined weekly using an *Orion* pH electrode/meter calibrated with certified NBS pH buffers of 4.01, 7.00, and 10.01.

The  $p\text{CO}_2$  for the four mixed gases employed in the experiments and the pH of the experimental seawaters were also measured at 1–2 h intervals over a 48-h period approximately midway through the 60-day experiment. The standard deviation of measured  $p\text{CO}_2$  and pH was less than 2 ppm and 0.001 pH units, respectively, for each of the four experimental seawater treatments throughout the 48-h interval. After water changes, the pH of the experimental seawaters returned to within 0.03 pH units of their average value in less than 3 h and returned completely to their average value within 5 h. This efficient mixing of the experimental seawaters and the experimental gases can be attributed to the rapid rate of gas bubbling that was employed ( $1 \text{ l min}^{-1}$ ), the use of ultra porous airstones specifically designed to promote gas–water equilibration, and the use of cellophane wrap to seal the tanks off from the ambient room air.

#### Calculated parameters (Table 1)

Total DIC,  $[\text{CO}_3^{2-}]$ ,  $[\text{HCO}_3^-]$ , dissolved  $\text{CO}_2$  ( $[\text{CO}_2]_{(\text{SW})}$ ), and  $p\text{CO}_2$  of the mixed gas in equilibrium with the experimental seawaters [ $p\text{CO}_2_{(\text{gas-e})}$ ] were calculated for each of the experimental seawaters from measured values of temperature, salinity, alkalinity, and pH using the program  $\text{CO}_2\text{SYS}$  (Lewis and Wallace 1998) with Roy et al. (1993) values for carbonic acid constants K1 and K2, Mucci (1983) value for the stoichiometric aragonite solubility product, and pressure = 1.015 atm. Variances reported for the calculated carbonate system parameters resulted primarily from fluctuations in seawater chemistry throughout the duration of the experiment, rather than from analytical uncertainty of the measured parameters. Differences among  $\Omega_A$  for the experimental seawaters equilibrated with the four  $p\text{CO}_2$  levels are statistically significant (student *t*-test,  $P < 0.05$ ) for each of the four tanks (Table 1). DIC was also measured once for each of the four seawater

treatments and compared to DIC values calculated from simultaneous measurements of pH and alkalinity. The average percent-error between the predicted and measured values of DIC was 2%. This suggests that the pH–alkalinity method employed for calculating the carbonate system parameters should be accurate, on average, to within 2% of the calculated values, which is less than the actual variation in pH and alkalinity throughout the duration of the experiment resulting from respiration, photosynthesis, and other biological activity within the aquaria (see Table 1).

#### Quantification of calcification rate

A buoyant weighing method (precision =  $\pm 0.3\%$ ; accuracy =  $\pm 1.1\%$ ) was employed to estimate the corals' rates of calcification (Davies 1989). At the beginning and end of the experiment, specimens were suspended at 15-cm depth in an aquarium filled with  $0.2 \mu\text{m}$ -filtered seawater ( $T = 25^\circ\text{C}$ ,  $\text{Sal} = 32$ ) by an aluminum wire hanging from a *Cole Parmer* bottom-loading scale. Measured changes in buoyant weight were generally on the order of hundreds or thousands of milligrams, well above the milligram precision of the scale. Calcification rates were calculated as the percent-change in buoyant weight between the beginning and end of the 60-day experiment, which helps control for allometric differences in growth rate by normalizing the coral specimens' 60-day calcification rates to their initial mass. Normalization of calcification rates to initial skeletal mass is not the optimal method for controlling for allometry in hermatypic corals with a low surface area-to-volume ratio (i.e., low tissue-to-skeleton ratio). The method is better suited for smaller ahermatypic corals, such as the species investigated here, for which the majority of their skeleton is immediately bordered by living tissue. The rate of calcification for these corals should vary relatively linearly as a function of their tissue area and, thus, their total skeletal mass. This is supported by the similarity between the calcification rate response patterns that were normalized to initial skeletal mass and the linear extension response patterns that were not.

The buoyant weighing method of estimating calcification or dissolution is limited by various factors, including the potential for unintended measurement of organic material attached to the skeleton that is of a density unequal to that of seawater. The buoyant weighing method for estimating dry  $\text{CaCO}_3$  weight was validated for the corals investigated in this study by plotting the corals' final buoyant weight against their final dry  $\text{CaCO}_3$  weight, which was estimated as the dry weight of the coral's skeleton after tissue was removed via combustion for 6 h at  $550^\circ\text{C}$  (Heiri et al. 2001). Buoyant weight and dry  $\text{CaCO}_3$  weight are highly correlated ( $R^2 = 0.99$ ,  $P < 0.0001$ ):

$$\text{Dry weight (mg)} = 1.61 * \text{Buoyant weight} + 33.78$$

Since the buoyant weight vs. dry weight regression is linear and passes near the origin, the percent-change in buoyant weight should be equivalent to the percent-change in dry weight.

Furthermore, because the buoyant weight calibration curves are based upon specimens that were actually employed in the experiments, any stochastic error arising from the buoyant weighing method (e.g., errors resulting from the measurement of tissue of a density unequal to that of seawater, from the geometry of the specimen, etc.) should be manifested as a deviation from the regressed calibration curve. Thus, the average percent-error of the  $\text{CaCO}_3$  vs. buoyant weight regressions should quantify the potential error imparted by any such complicating factors. This error is about 1.1%. Given the excellent correlation ( $R^2 = 0.99$ ,  $P < 0.0001$ ) between buoyant weight and dry  $\text{CaCO}_3$  weight observed for the corals investigated in this study and the need to make nondestructive determinations of skeletal mass at the beginning of the experiment, buoyant weighing constitutes a viable method for estimating rates of coral calcification under these experimental conditions.

#### Measurement of linear extension relative to a $^{137}\text{Ba}/^{138}\text{Ba}$ skeletal time maker

Each aquarium was dosed with  $0.49 \text{ mg } ^{137}\text{BaCO}_3$  for 14 days at the beginning of the 60-day experiment. This addition of  $^{137}\text{BaCO}_3$  effectively quintupled the concentration of  $^{137}\text{Ba}$  in the experimental seawaters, while only increasing the total Ba concentration in the seawater by  $\sim 45\%$ . After 14 days, the  $^{137}\text{Ba}$ -enriched experimental seawaters were replaced with experimental seawaters of natural Ba isotopic composition. The temporary increase in concentration of  $^{137}\text{Ba}$  (relative to the more abundant  $^{138}\text{Ba}$ ) in the experimental seawaters resulted in an approximately fivefold spike in the  $^{137}\text{Ba}/^{138}\text{Ba}$  ratio in the coral skeletons accreted during the first 14 days of the experiment (Fig. 1). This spike served as a time marker that identified skeletal material accreted under the experimental conditions and provided a baseline from which linear extension of the coral skeleton could be measured.

Four coral specimens were randomly selected from each of the experimental seawater treatments and sectioned through their apical corallites (parallel to their growth axes) using a high-precision circular trim tool.  $^{137}\text{Ba}/^{138}\text{Ba}$  ratios were measured at a constant scan rate along the growth axis of the apical corallite's septal wall using laser ablation-inductively coupled plasma-mass spectrometry (*ThermoFinnigan Element2* LA-ICP-MS; beam diameter =  $5 \mu\text{m}$ ; scan speed =  $6 \mu\text{m}/\text{sec}$ ; intensity = 35%; frequency 8 Hz).

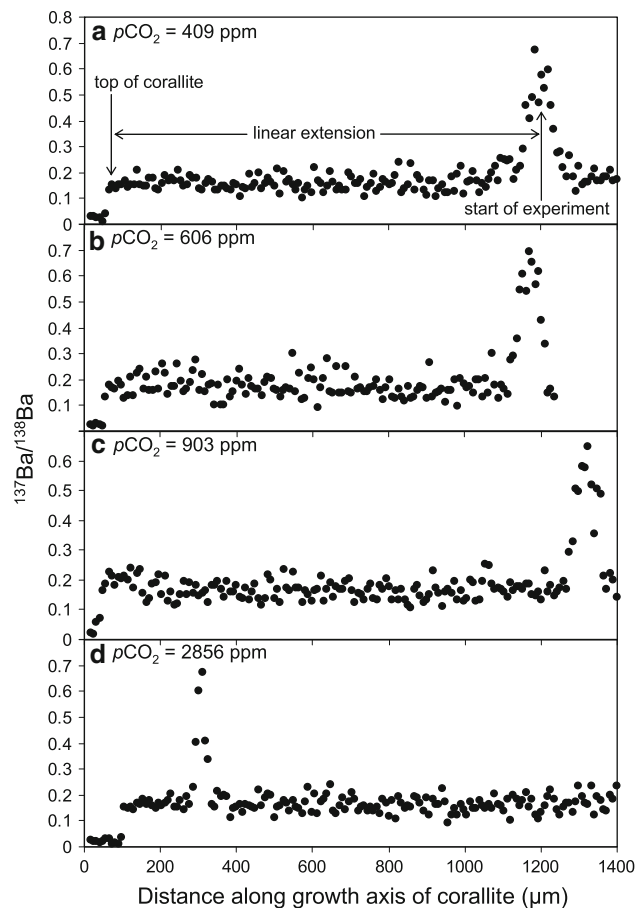


**Fig. 1** Examples of the  $^{137}\text{Ba}/^{138}\text{Ba}$  isotope data obtained along the growth axes of coral specimens reared in the 409 (a), 606 (b), 903 (c), and 2,856 (d) ppm  $p\text{CO}_2$  treatments. Isotope spikes mark the beginning of the 60-day experiment. Linear extension was measured as the distance between the  $^{137}\text{Ba}/^{138}\text{Ba}$  isotope spike and the top of the corallite (marked by loss of the  $^{137}\text{Ba}/^{138}\text{Ba}$  signal) for corals reared in each of the four experimental seawater treatments

The time that elapsed between detection of the  $^{137}\text{Ba}/^{138}\text{Ba}$  spike and the outer edge of the coral skeleton was converted to distance by multiplying this elapsed time by the scan rate of the laser (Fig. 1). Unlike calcification rate, rate of linear extension should not vary with the size of the colony and was therefore not normalized to initial skeletal mass.

#### Statistical treatment of the calcification and linear extension data

Linear, quadratic, and exponential regression analyses, calculated using the least-squares method, were used to assess the relationship between aragonite saturation state of the experimental seawater and rates of calcification (Fig. 2) and linear extension (Fig. 3). The regression analysis (linear, quadratic, or exponential) that was statistically significant ( $P < 0.05$ ) and that yielded the least root mean squared error (RMSE) was employed to describe the

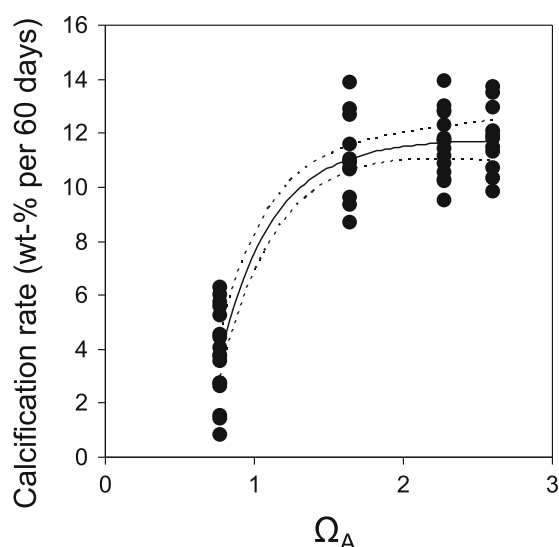


**Fig. 2** Calcification rate vs.  $\Omega_A$  for *Oculina arbuscula* specimens reared for 60 days in experimental seawater treatments. Calcification rates are estimated from buoyant weighing (verified with dry weight measured postharvesting) and expressed as a percentage of the organisms' initial buoyant weight (see Table 3).  $\Omega_A = [\text{Ca}^{2+}][\text{CO}_3^{2-}]/K_{sp}^*$ , where  $K_{sp}^*$  is the stoichiometric solubility product of aragonite.  $\Omega_A$  was calculated from measured values of temperature, salinity, alkalinity, and pH (see Table 1) with the program CO<sub>2</sub>SYS (Lewis and Wallace 1998) using Roy et al. (1993) values for carbonic acid constants K1 and K2, Mucci (1983) value for the stoichiometric aragonite solubility product, and  $P = 1.015$  atm. Relationship between calcification rate and  $\Omega_A$  was assessed with linear, quadratic, and exponential regressions (see text for details). The exponential regression (solid curve) is plotted above because it was statistically significant ( $P < 0.05$ ) and yielded the lowest RMSE. Dashed curves correspond to the 95% confidence interval of the regression, which denotes that there is a 95% probability that the regression that accurately describes the relationship between calcification rate and  $\Omega_A$  falls within this interval. Regression curve is intended to show general trend; the location of the break-in-slope of the curve is not precisely constrained by the available data

relationship between seawater saturation state with respect to aragonite and the calcification (Fig. 2) and linear extension data (Fig. 3).

Intercolonial variation was controlled for by rearing coral specimens from 19 different colonies in each of the experimental seawater treatments. However, these nineteen specimens were all reared in the same aquarium for a given treatment. This form of pseudo-replication (Hurlbert 1984) increases the possibility that the response of specimens reared under a given treatment would be more closely distributed about a mean value than if they had each been reared in separate, replicated treatments. This so-called clustering could potentially reduce the variance of the measurements of specimens reared under a given treatment, thereby artificially increasing the likelihood that a regression through the data would pass a test for significance that is based upon a model of normal probability distribution. Nevertheless, when resources are limited, the inferential

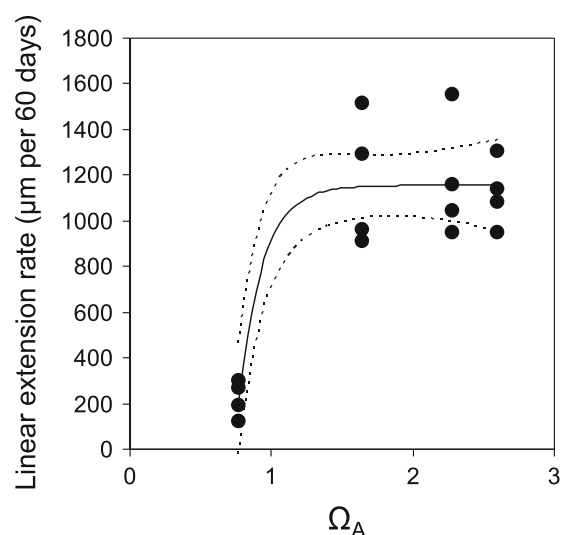


**Fig. 3** Linear extension rate vs.  $\Omega_A$  for sixteen randomly selected *Oculina arbuscula* specimens reared for 60 days in the experimental seawater treatments. Rates of linear extension (Table 4) are measured relative to a  $^{137}\text{Ba}/^{138}\text{Ba}$  skeletal time marker emplaced at the start of the experiment (Fig. 1). Relationship between linear extension rate and  $\Omega_A$  was assessed with linear, quadratic, and exponential regressions (see text for details). The exponential regression (solid curve) is plotted above because it was statistically significant ( $P < 0.05$ ) and yielded the lowest RMSE. Dashed curves correspond to the 95% confidence interval of the regression, which denotes that there is a 95% probability that the regression that accurately describes the relationship between linear extension rate and  $\Omega_A$  falls within this interval. Regression curve is intended to show general trend; the location of the break-in-slope of the curve is not precisely constrained by the available data

power that is gained by employing additional treatment levels at the expense of treatment replication may, in some cases, justifies the use of a pseudo-replicated study design (for discussion, see Hawkins 1986; Barry et al. 2009).

This potential clustering associated with the pseudo-replicated experimental design was controlled for by employing Generalized Estimating Equations that employ the Huber-White sandwich estimator of variance, also known as the Robust Covariance Matrix, in place of the standard estimator of variance (Rogers 1993). Essentially, instead of employing statistical parameters that assume that the data will be normally distributed about the mean (via the standard estimator of variance), the Huber-White estimator of variance uses a Taylor Series Expansion to adjust the statistical parameters so that they are based on the actual distribution of the data in each of the tanks. This conservative approach minimizes the likelihood of committing a type 1 statistical error as a result of the pseudo-replicated experimental design.

#### Microimaging of coral skeleton

Prior to combustion of organic matter, one coral specimen from each of the experimental seawater treatments was

broken parallel to its growth axis with forceps and then carbon coated for  $\sim 30$  s. The portion of skeleton accreted under the experimental conditions (determined relative to the  $^{137}\text{Ba}/^{138}\text{Ba}$  spike) was then imaged with a *JEOL 840* scanning electron microscope.

### Mineralogical analysis

The polymorph mineralogy of the  $\text{CaCO}_3$  precipitated by the corals was determined by powder X-ray diffraction (XRD). Skeletal material accreted under the experimental conditions (determined relative to the  $^{137}\text{Ba}/^{138}\text{Ba}$  spike) was extracted by scalpel under a stereomicroscope from the sixteen corals (four from each treatment) that were analyzed for the  $^{137}\text{Ba}/^{138}\text{Ba}$  spike. This material was mixed with  $\sim 10$  drops of 95% ethyl alcohol and gently ground for 2 min into a fine powder using an agate mortar and pestle. The slurry was then injected into a 1 cm  $\times$  1 cm  $\times$  10  $\mu\text{m}$  reservoir on a glass slide and allowed to dry overnight. The equally thick layer of  $\text{CaCO}_3$  crystals that resulted from this preparation was analyzed for polymorph mineralogy using powder XRD. The proportion of aragonite-to-calcite was calculated from the ratio of the area under the primary aragonite peak [d(111): 3.39 Å;  $2\theta = 26.3^\circ$ ] to the area under the primary calcite peak [d(104): 2.98–3.03 Å;  $2\theta = 29.5\text{--}30.0^\circ$ ], using standardized mixtures to calibrate this relationship (precision = 1.5%; calcite detectable at a minimum of 3 mol%).

## Results

### Survivorship

During the acclimation phase, prior to the start of the experiment, survivorship of the coral specimens varied among the treatments but was not significantly correlated with either  $\Omega_A$  ( $R^2 = 0.49$ ,  $P > 0.05$ ), subsequent average calcification rate ( $R^2 = 0.61$ ,  $P > 0.05$ ), or subsequent average rate of linear extension ( $R^2 = 0.58$ ,  $P > 0.05$ ).

Whatever factor was responsible for the initial mortality during the acclimation phase did not systematically influence the corals' rates of calcification or linear extension. Following the initial acclimation phase, survivorship in each experimental treatment was 100%.

### Calcification rates

Average rates of calcification ( $\pm\text{SD}$ ) for the corals reared under  $\Omega_A$  of 2.6, 2.3, 1.6, and 0.8 were 11.8 ( $\pm 1.2$ ), 11.6 ( $\pm 1.2$ ), 11.1 ( $\pm 1.5$ ), and 3.8 ( $\pm 1.7$ ) % per 60 days (Fig. 2, Tables 2, 3). The relationship between  $\Omega_A$  and calcification rate was assessed with linear ( $y = 4.56x + 1.19$ ;  $P = 0.01$ ,  $R^2 = 0.74$ ,  $\text{RMSE} = 1.97$ ), quadratic ( $y = -3.93x^2 + 17.4x - 7.22$ ;  $P = 0.00$ ;  $R^2 = 0.86$ ;  $\text{RMSE} = 1.46$ ), and exponential regressions ( $y = -67.2e^{-2.77x} + 11.8$ ;  $P = 0.00$ ;  $R^2 = 0.87$ ;  $\text{RMSE} = 1.43$ ). The exponential regression was employed to quantify this relationship (Fig. 2) because it was statistically significant ( $P < 0.05$ ) and yielded the lowest RMSE. However, no statistically significant ( $P < 0.05$ ) change in calcification rate was observed between  $\Omega_A$  of 2.6 and 1.6.

### Rates of linear extension

Average rates of linear extension for the corals reared under  $\Omega_A$  of 2.6, 2.3, 1.6, and 0.8 were 1.1 ( $\pm 0.15$ ), 1.2 ( $\pm 0.26$ ), 1.2 ( $\pm 0.29$ ), and 0.2 ( $\pm 0.08$ ) mm per 60 days (Fig. 3, Tables 2, 4). The relationship between  $\Omega_A$  and linear extension rate was assessed with linear ( $Y = 491.6x + 24.85$ ;  $P = 0.05$ ,  $R^2 = 0.60$ ,  $\text{RMSE} = 302.0$ ), quadratic ( $y = 2499x^2 - 601.8x - 1340$ ;  $P = 0.00$ ;  $R^2 = 0.82$ ;  $\text{RMSE} = 207.7$ ), and exponential regressions ( $y = -87642e^{-5.8964x} + 1156.0$ ;  $P = 0.00$ ;  $R^2 = 0.83$ ;  $\text{RMSE} = 198.5$ ). The exponential regression was employed to quantify this relationship (Fig. 3) because it was statistically significant ( $P < 0.05$ ) and yielded the lowest RMSE. However, no statistically significant ( $P < 0.05$ ) change in linear extension rate was observed between  $\Omega_A$  of 2.6 and 1.6.

**Table 2** Average aragonite saturation state ( $\Omega_A$ ), average calcification rate obtained from buoyant weighing, and average linear skeletal extension rate measured relative to a  $^{137}\text{Ba}/^{138}\text{Ba}$  isotopic time

$\Omega_A$	Calcification (wt%/60-day, AVG)	SD	Range	<i>n</i>	Linear extension ( $\mu\text{m}/60\text{-day}$ , AVG)	SD	Range	<i>n</i>
2.60	11.8	1.2	9.8–13.7	11	1,117	149	946–1,306	4
2.28	11.6	1.2	9.5–13.9	15	1,176	263	950–1,550	4
1.64	11.1	1.5	8.7–13.9	12	1,169	287	909–1,516	4
0.77	3.8	1.7	0.8–6.3	17	220	81	119–301	4

marker added at the start of the experiment. “SD” is standard deviation; “*n*” is sample size

**Table 3** Detailed buoyant and dry weight data for *Oculina arbuscula* investigated in the experiment. Initial and final weights refer to weight at the beginning and end of the experiment. Corals' dry weight of CaCO<sub>3</sub> is estimated from its buoyant weight using the empirically derived calibration curve

Sample ID	$\Omega_A$	Buoyant weight		Dry weight of CaCO <sub>3</sub>	
		Initial (mg)	Final (mg)	Initial (mg)	Final (mg)
A01	2.60	1,463	1,620	2,393	2,645
A02	2.60	1,790	1,966	2,920	3,203
A03	2.60	1,446	1,618	2,364	2,642
A04	2.60	1,999	2,225	3,256	3,620
A05	2.60	1,294	1,468	2,119	2,400
A06	2.60	2,961	3,318	4,807	5,382
A07	2.60	2,644	2,917	4,296	4,736
A08	2.60	2,505	2,830	4,072	4,596
A09	2.60	2,402	2,686	3,906	4,364
A10	2.60	2,007	2,282	3,269	3,712
A11	2.60	3,403	3,793	5,520	6,148
B01	2.28	1,668	1,863	2,722	3,036
B02	2.28	1,424	1,579	2,330	2,580
B03	2.28	1,884	2,106	3,071	3,428
B04	2.28	2,394	2,647	3,893	4,300
B05	2.28	3,964	4,340	6,424	7,030
B06	2.28	1,370	1,545	2,243	2,525
B07	2.28	1,763	1,965	2,876	3,201
B08	2.28	3,192	3,548	5,179	5,752
B09	2.28	1,906	2,131	3,106	3,469
B10	2.28	2,284	2,518	3,716	4,092
B11	2.28	1,623	1,831	2,650	2,985
B12	2.28	1,958	2,212	3,190	3,600
B13	2.28	2,644	3,012	4,296	4,889
B14	2.28	3,269	3,670	5,303	5,950
B15	2.28	1,302	1,436	2,133	2,348
C01	1.64	1,989	2,180	3,240	3,548
C02	1.64	1,727	1,916	2,818	3,122
C03	1.64	2,346	2,604	3,815	4,231
C04	1.64	1,180	1,329	1,935	2,176
C05	1.64	2,174	2,377	3,538	3,866
C06	1.64	1,704	1,885	2,780	3,072
C07	1.64	1,571	1,742	2,566	2,842
C08	1.64	1,677	1,857	2,737	3,027
C09	1.64	1,802	2,034	2,939	3,313
C10	1.64	2,145	2,443	3,492	3,972
C11	1.64	2,617	2,919	4,252	4,739
C12	1.64	1,912	2,078	3,116	3,384
D01	0.77	2,082	2,177	3,391	3,543
D02	0.77	1,661	1,765	2,711	2,879
D03	0.77	1,607	1,668	2,625	2,723
D04	0.77	1,851	1,902	3,018	3,100

**Table 3** continued

Sample ID	$\Omega_A$	Buoyant weight		Dry weight of CaCO <sub>3</sub>	
		Initial (mg)	Final (mg)	Initial (mg)	Final (mg)
D05	0.77	2,200	2,231	3,580	3,630
D06	0.77	1,822	1,837	2,971	2,995
D07	0.77	2,368	2,430	3,850	3,951
D08	0.77	1,815	1,895	2,960	3,089
D09	0.77	1,717	1,787	2,802	2,914
D10	0.77	2,170	2,250	3,532	3,661
D11	0.77	1,833	1,884	2,989	3,071
D12	0.77	2,354	2,495	3,828	4,056
D13	0.77	2,651	2,803	4,308	4,552
D14	0.77	2,096	2,170	3,412	3,532
D15	0.77	1,329	1,349	2,176	2,208
D16	0.77	1,872	1,977	3,052	3,221
D17	0.77	1,977	2,080	3,220	3,387

**Table 4** Detailed linear extension data for four randomly selected *Oculina arbuscula* specimens selected from each of the four experimental seawater treatments. Linear extension was measured relative to a <sup>137</sup>Ba/<sup>138</sup>Ba skeletal time marker emplaced at the start of the experiment

Sample ID	$\Omega_A$	Linear extension (μm/60-days)
A01	2.60	1,306
A06	2.60	1,079
A07	2.60	946
A09	2.60	1,137
B02	2.28	950
B04	2.28	1,158
B06	2.28	1,550
B09	2.28	1,046
C02	1.64	909
C05	1.64	959
C09	1.64	1,294
C10	1.64	1,516
D07	0.77	119
D12	0.77	301
D13	0.77	269
D16	0.77	193

#### Skeletal mineralogy

Powder XRD patterns for each of the 16 coral skeletons analyzed (not shown) revealed a strong aragonite peak and no calcite peak. This indicates that aragonite was the only form of crystalline CaCO<sub>3</sub> secreted by the corals under each of the four aragonite saturation states.

## Discussion

### Nonlinear response to CO<sub>2</sub>-induced ocean acidification

The *O. arbuscula* corals investigated in the present study exhibited a nonlinear response in their rates of calcification and linear extension, such that no significant ( $P < 0.05$ ) difference was detected relative to the control treatment ( $\Omega_A = 2.6$ ) for corals reared under  $\Omega_A$  of 2.3 and 1.6, while a strong negative response was observed for corals reared under the  $\Omega_A$  of 0.8. The backscatter electron images (Fig. 4) revealed no evidence of localized dissolution, such as cross-cutting dissolution surfaces. This suggests that the decline in calcification and linear extension in

undersaturated conditions ( $\Omega_A = 0.8$ ; Fig. 4d) was caused not by localized or intermittent dissolution of the coral skeleton, but rather by a true decline in the rate of mineral accretion at the coral's site of calcification.

The observation that the *O. arbuscula* corals exhibited no change in their rates of calcification and linear extension until  $\Omega_A$  was reduced to 0.8 ( $\pm 0.07$ ) is consistent with our hypothesis that there exists a threshold  $\Omega_A$  that these corals can tolerate before exhibiting any major reduction in calcification. When  $\Omega_A$  remains above this critical value, calcification and linear extension are relatively unimpaired by changes in carbonate chemistry. However, when  $\Omega_A$  exceeds this threshold value, there appears to be a negative impact on both calcification and linear extension. The

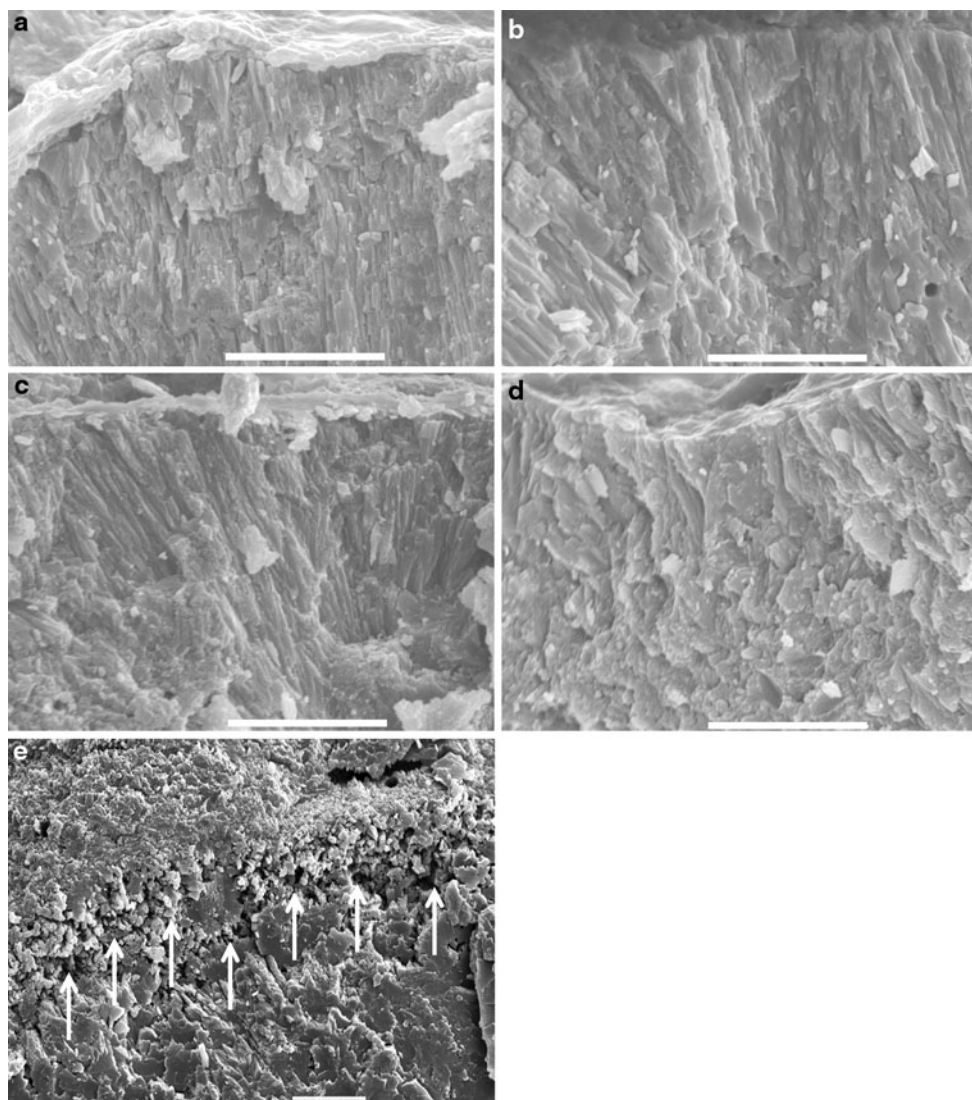


**Fig. 4** Backscatter electron images of cleaved sections of the aragonite skeletons accreted by *Oculina arbuscula* specimens in experimental seawaters formulated at  $\Omega_A$  of 2.6 (a), 2.3 (b), 1.6 (c), and 0.8 (d), which contain no evidence of localized dissolution surfaces. A backscatter electron image of an *Astrangia poculata* coral

that developed a localized dissolution surface (arrows) during a 2-day exposure to seawater of pH 6.8 (overlain by additional skeleton accreted in normal pH seawater) is included for comparison (e). Scale bar is 10  $\mu\text{m}$

precise value of this potential threshold  $\Omega_A$  is not well-constrained by the current data set, which indicates only a threshold value somewhere between 0.8 and 1.6. These results are important, nonetheless, because they suggest that although corals' response may be weak or even non-existent in the early stages of ocean acidification, they may exhibit a more negative response once their threshold is surpassed.

One possible explanation for the nonlinear response in calcification is that corals are able to control the carbonate chemistry of their calcifying fluid equally well under all four treatments and that the abrupt reduction in calcification resulted from the dissolution of exposed portions of the coral skeleton in the undersaturated conditions, despite a constant rate of calcification beneath the corals' tissue. This explanation appears unlikely for two reasons. First, none of the corals investigated in the present study lost enough tissue for their skeletons to ever be in direct contact with ambient seawater, and all specimens were attached to acrylic slides with a thick band of cyanoacrylate that effectively sealed off the exposed base of the coral fragment. Second, and perhaps more importantly, the nonlinear responses were observed for both calcification and linear extension. If localized dissolution of exposed coral skeleton was the primary cause of the nonlinear reduction in calcification rate, then one would not expect to see a similar nonlinear pattern also manifest in the linear extension data. This is because the linear extension measurements were obtained from portions of the skeleton that were covered with living tissue throughout the duration of the experiment. However, the calcification and linear extension data were highly linearly correlated ( $R^2 = 0.72$ ,  $P < 0.005$ ; Fig. 5), both exhibiting nonlinear responses of a similar form. This suggests that the nonlinear reductions in calcification and linear extension were actually caused by a decline in the rate of mineral accretion at the coral's site of calcification, rather than by localized dissolution of exposed skeleton. The absence of any obvious dissolution line or visible crystal damage in the SEM images in Fig. 4d supports this interpretation.

We propose that the apparent insensitivity of calcification and linear extension within *O. arbuscula* to reductions in  $\Omega_A$  from 2.6 to 1.6 reflects the corals' ability to manipulate the carbonate chemistry at their site of calcification. Their negative response to  $\Omega_A = 0.8$  suggests that there may be a limit on that ability. Scleractinian corals are thought to facilitate precipitation of skeletal aragonite by elevating  $\Omega_A$  of the calcifying medium between their skeleton and calcicoblastic epithelium (Cohen and McConnaughey 2003). Although actual data on the composition of the calcifying medium is limited and deduced largely from proxy measurements of crystal chemistry and morphology (e.g., Gaetani and Cohen 2006; Cohen et al. 2009; Cohen

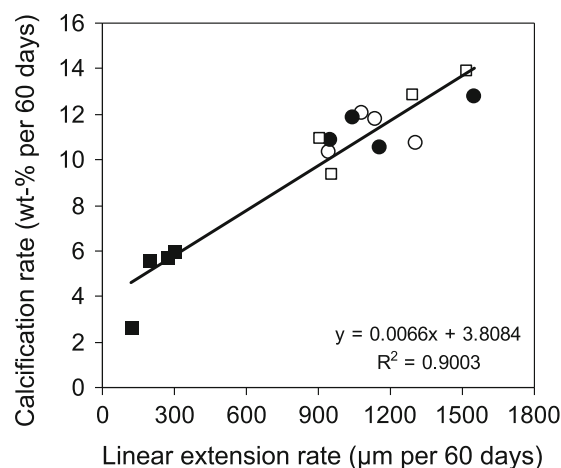


**Fig. 5** Linear extension rates vs. calcification rates for corals reared under the four experimental seawater treatments for which both of these parameters were measured. Linear regression was calculated using the least-squares method. Open circles, closed circles, open squares, and closed squares correspond to corals reared under  $\Omega_A$  of 2.6, 2.3, 1.6, and 0.8, respectively

and Holcomb 2009), there is one set of in situ microelectrode data, reportedly from the calcifying space, that shows significantly elevated pH (up to 9.3 in the light) in the tropical scleractinian coral *Galaxea fascicularis*, compared with ambient seawater pH of 8.2 (Al-Horani et al. 2003). If corals indeed elevate  $\Omega_A$  of the calcifying medium by elevating its pH, there are a number of ways they could achieve this, including via  $\text{Ca}^{2+}$ -proton ATPase, direct proton pumping, transcellular proton-solute shuttling, and  $\text{CO}_2$  utilization via zooxanthellate photosynthesis (McConnaughey and Whelan 1997; Al-Horani et al. 2003; Cohen and McConnaughey 2003). Corals could also elevate  $\Omega_A$  of the calcifying medium without necessarily increasing its pH by, for instance, elevating total DIC via respiration and/or  $\text{HCO}_3^-$  transport and then pumping the liberated protons out of the calcifying medium. This may be why calcification within some corals is stimulated by the addition of  $\text{HCO}_3^-$  (e.g., Marubini and Thake 1999; Herfort et al. 2008; Jury et al. 2009). The observation that *O. arbuscula* exhibited comparable rates of calcification and linear extension under  $\Omega_A$  of 2.6, 2.3, and 1.6 suggests that, under the given experimental conditions, *O. arbuscula* was able to maintain a suitably elevated  $\Omega_A$  at the calcification site despite reductions in external  $\Omega_A$ . However, when  $\Omega_A$  of the external seawater environment becomes sufficiently low (e.g., below 1.6 for *O. arbuscula* in this study), it is likely that the coral's ability to remove protons from the calcifying medium (i.e., convert  $\text{HCO}_3^-$  to  $\text{CO}_3^{2-}$ ) can no longer offset the unfavorable external conditions, resulting in the observed decline in calcification.

The nonlinear calcification response by *O. arbuscula* to reduced  $\Omega_A$  may also be partly attributable to the fact that

this coral obtains some of its nourishment from photosynthetic zooxanthellate endosymbionts hosted within its epithelial tissue. It is possible that the deleterious effects of the more moderate CO<sub>2</sub>-induced reductions in  $\Omega_A$  (2.6–1.6) were partially offset by CO<sub>2</sub>-fertilization of these endosymbionts, which may have transferred additional energy to the coral, thereby enhancing its ability to manipulate the carbonate chemistry of its calcifying medium under moderately elevated  $p\text{CO}_2$ . If this occurred, then the benefit of enhanced photosynthesis must have ultimately been offset by the cost of calcifying in undersaturated conditions ( $\Omega_A = 0.8$ ), as evidenced by the decline in calcification and linear extension that occurred under these conditions.

Although the general nonlinearity of the response of *O. arbuscula* to elevated  $p\text{CO}_2$  under the given experimental conditions (temperature, nutrients, etc.) can be deduced with relative confidence, the experimental design (e.g., lack of  $p\text{CO}_2$  treatment levels between 903 and 2,856 ppm, pseudo-replication, weekly—rather than daily—monitoring of carbonate system parameters) precludes identification of the precise location of the break-in-slope (or perhaps, a more gradual change in slope) that characterizes the apparent nonlinearity. Future efforts to constrain this nonlinearity should utilize more highly controlled and replicated experiments designed to investigate the responses of multiple species of scleractinian corals reared (preferably side-by-side) under more incrementally elevated levels of atmospheric  $p\text{CO}_2$  and under various nutrient and temperature regimes.

#### Production of new skeletal material in undersaturated conditions

Rates of calcification and linear extension for *O. arbuscula* were positive in each of the experimental seawater treatments. Thus, even in seawater that is undersaturated with respect to aragonite, the corals were still able to accrete new skeletal material. These results agree with earlier experiments showing that the cold water coral *L. pertusa* (Maier et al. 2009) and larvae of the tropical coral *Favia fragum* (Cohen et al. 2009) are able to continue accreting new skeletal aragonite in undersaturated conditions. These observations are consistent with the hypothesis that corals exert strong control over the composition of their calcifying fluid (McConnaughey and Whelan 1997; Al-Horani et al. 2003; Cohen and McConnaughey 2003). If crystal nucleation and growth were controlled only by organic templates and not by elevating  $\Omega_A$  of the coral's calcifying medium, then we might expect that their aragonite skeleton would dissolve after nucleation under the high  $p\text{CO}_2$  treatment (2,850 ppm,  $\Omega_A < 1.0$ ). Rather, we suggest that the corals are able to manipulate the carbonate chemistry of their calcifying medium so that not only does aragonite

nucleate, but it continues to accrete at a measurable rate (i.e., total calcification > total dissolution)—albeit slower than in seawater treatments maintained at higher  $\Omega_A$  (Figs. 2, 3).

The ability of *O. arbuscula* corals to accrete aragonite in seawater of pH 7.48 contrasts with the Fine and Tchernov (2007) study that reported complete skeletal dissolution for the Mediterranean corals *Oculina patagonica* and *Madracis pharencis* reared in seawater of pH 7.3–7.6. However, Fine and Tchernov (2007) manipulated seawater pH through acid addition (reduced pH, reduced alkalinity, and reduced DIC), while the present study manipulated seawater pH by bubbling seawater with CO<sub>2</sub>-air mixtures (reduced pH, increased DIC, constant alkalinity; Cohen et al. 2009; Schulz et al. 2009). Thus, the method employed by Fine and Tchernov yielded a substantially lower concentration of carbonate and bicarbonate ions than was maintained under the highest  $p\text{CO}_2$  treatment (2,856 ppm) employed in the present study, despite maintaining approximately equivalent seawater pH.

#### Precipitation of the aragonite polymorph under each of the four treatments

Prior work has shown that three species of tropical, reef-building scleractinian corals, *Porites cylindrica*, *Montipora digitata*, and *Acropora cervicornis*, accreted nearly one-third of their skeleton as the hexagonal calcite polymorph of CaCO<sub>3</sub>, rather than their normal orthorhombic aragonite polymorph, when reared in experimental seawater formulated with a Mg/Ca ratio favoring the abiotic precipitation of calcite (molar Mg/Ca = 1.0; so-called “calcite seawater”; Ries et al. 2006). This apparent plasticity in coral polymorph mineralogy raised the possibility that corals reared in CO<sub>2</sub>-acidified experimental seawaters that were simultaneously undersaturated with respect to aragonite yet oversaturated with respect to calcite ( $p\text{CO}_2 = 2,856$  ppm;  $\Omega_A = 0.8$ ;  $\Omega_{\text{calcite}} = 1.2$ ) would also begin producing a portion of their skeleton as the less soluble calcite polymorph. However, the observation that *O. arbuscula* secreted exclusively the aragonite polymorph of CaCO<sub>3</sub> under each of the four  $\Omega_A$  treatments suggests that this coral is unlikely to adapt to elevated  $p\text{CO}_2$  by producing a less soluble form of CaCO<sub>3</sub> in response to CO<sub>2</sub>-induced ocean acidification.

#### Variable responses to CO<sub>2</sub>-induced ocean acidification among coral species and experimental conditions

Data generated from several experimental studies (e.g., Marubini and Atkinson 1999; Marubini et al. 2001, 2003, 2008; Langdon and Atkinson 2005; Schneider and Erez 2006) and compiled by several review papers (e.g.,

Langdon et al. 2000; Langdon and Atkinson 2005) have been interpreted as evidence that corals exhibit linearly negative calcification responses to CO<sub>2</sub>-induced ocean acidification. However, the results of the present study on the temperate coral *O. arbuscula*, in conjunction with the results of other experimental studies on a range of temperate and tropical corals (Reynaud et al. 2003; Ries et al. 2009; Jury et al. 2009; Cohen et al. 2009; Rodolfo-Metalpa et al. 2010; Holcomb et al. 2010), suggest that the coral calcification response to ocean acidification may be more complex.

Reynaud et al. (2003) showed that the tropical coral *Stylophora pistillata* exhibited no change in calcification rate when atmospheric pCO<sub>2</sub> was elevated from 450 to 738 ppm at 25°C, although a decline in calcification was observed at 28°C. Houlbreque et al. (pers. comm.) observed no calcification response for this tropical species down to pH = 7.5. Jury et al. (2009) also showed that the tropical coral *Madracis auretenra* exhibited no statistically significant difference in calcification rate when reared under atmospheric pCO<sub>2</sub> of 393, 876, and 1,406 ppm. Cohen et al. (2009) observed that new recruits of the slow-growing tropical coral *Favia fragum* exhibited a parabolic-negative response to HCl-induced reductions in Ω<sub>A</sub> from 3.7 to 2.4 to 1.0 to 0.2. However, de Putron et al. (pers. comm.) reported no statistically significant response to CO<sub>2</sub>-induced reductions in Ω<sub>A</sub> for new recruits of *F. fragum* and the fast-growing tropical species *Porites astreoides* until Ω<sub>A</sub> = 1.5.

Rodolfo-Metalpa et al. (2010) showed that the temperate coral *Cladocora caespitosa* exhibited no statistically significant difference in calcification rate when reared in experimental seawaters bubbled with CO<sub>2</sub>-air mixtures of ca. 400 and 700 ppm pCO<sub>2</sub>. They did report, however, that seasonal changes in temperature had a statistically significant impact on rates of photosynthesis and calcification. Likewise, Holcomb et al. (2010) observed that the temperate coral *Astrangia poculata* exhibited no statistically significant difference in calcification rate when reared in seawaters bubbled with air-CO<sub>2</sub> mixtures of ca. 386 and 780 ppm pCO<sub>2</sub> under elevated nutrient concentrations. However, a sharp decline in calcification was observed between 386 and 780 ppm pCO<sub>2</sub> under normal nutrient concentrations (Vineyard Sound seawater). They also noted (pers. comm.) that it was only the spawning females that exhibited a negative response to 780 ppm pCO<sub>2</sub>—males and nonspawning females showed no response.

The present study on *O. arbuscula* augments the growing body of evidence that corals' response to elevated atmospheric pCO<sub>2</sub> is variable and complex. The disparate responses observed for corals in ocean acidification experiments appear to arise not only from fundamental differences among species, but also from differences

among experimental conditions, including temperature, method of acidification (CO<sub>2</sub> v. HCl), nutrient level, and polyp age. Although no statistically significant change in calcification was observed for *O. arbuscula* between Ω<sub>A</sub> of 2.6 and 1.6 in the present study, a substantial reduction was observed at Ω<sub>A</sub> = 0.8. It is therefore critical that the relative insensitivity of this species to moderate reductions in Ω<sub>A</sub> (2.6–1.6) not belie their apparent vulnerability to more severe reductions in Ω<sub>A</sub>.

**Acknowledgments** We are grateful to Greg Piniak at NOAA in Beaufort, North Carolina, for generously collecting and supplying the coral specimens used in this study. We thank Wade McGillis for providing gas standards. Michael Holcomb provided critical input in the design and implementation of these experiments. This work was supported with funding from UNC—Chapel Hill (to JBR), the Ocean and Climate Change Institute at WHOI (to JBR), the Tropical Research Institute at WHOI (to ALC), and the National Science Foundation (to ALC and DCM).

## References

- Al-Horani FA, Al-Moghrabi SM, DeBeer D (2003) The mechanism of calcification and its relation to photosynthesis and respiration in the scleractinian coral *Galaxea fascicularis*. *Mar Biol* 142:419–426
- Barry J, Tyrrell T, Hansson L, Gattuso J-P 2009, Section 2.1: Atmospheric CO<sub>2</sub> targets for ocean acidification perturbation experiments. In: Riebesell U, Fabry VJ, Gattuso J-P (eds) Guide to best practices for ocean acidification research. <http://www.epoca-project.eu/index.php/Home/Guide-to-OA-Research/>
- Brewer PG (1997) Ocean chemistry of the fossil fuel CO<sub>2</sub> signal: The haline signal of “business as usual”. *Geophys Res Lett* 24: 1367–1369
- Cohen AL, Holcomb MC (2009) Why corals care about ocean acidification: uncovering the mechanism. *Oceanography* 22: 118–127
- Cohen AL, McConnaughey TA (2003) A geochemical perspective on coral mineralization. In: Dove PM, Weiner S, De Yoreo JJ (eds) Biom mineralization. *Reviews in Mineralogy and Geochemistry* 54: 151–187
- Cohen AL, McCorkle DC, de Putron S, Gaetani GA, Rose KA (2009) Morphological and compositional changes in the skeletons of new coral recruits reared in acidified seawater: Insights into the biom mineralization response to ocean acidification. *Geochim Geophys Res Lett* 36:Q07005
- Davies PS (1989) Short-term growth measurements of corals using an accurate buoyant weighing technique. *Mar Biol* 101:389–395
- Doney SC, Schimel DS (2007) Carbon and climate system coupling on timescales from the Precambrian to the Anthropocene. *Annu Rev Environ Resour* 32:31–66
- Doney SC, Fabry VJ, Feely RA, Kleypas JA (2009) Ocean acidification: the other CO<sub>2</sub> problem. *Annu Rev Mar Sci* 1:169–192
- Fabry VJ, Seibel BA, Feely RA, Orr JC (2008) Impacts of ocean acidification on marine fauna and ecosystem processes. *ICES J Mar Sci* 65:414–432
- Fine M, Tchernov D (2007) Scleractinian coral species survive and recover from decalcification. *Science* 315:1811
- Gaetani GA, Cohen AL (2006) Element partitioning during precipitation of aragonite from seawater: A framework for understanding paleoproxies. *Geochim Cosmochim Acta* 70:4617–4634

- Hawkins CP (1986) Pseudo-understanding of pseudoreplication: A cautionary note. *Bull Ecol Soc Am* 67:184–185
- Heiri OO, Lotter AF, Lemcke G (2001) Loss on ignition as a method for estimating organic and carbonate content in sediments: reproducibility and comparability of results. *J Paleolimnol* 25:101–110
- Herfort L, Thake B, Taubner I (2008) Bicarbonate stimulation of calcification and photosynthesis in two hermatypic corals. *J Phycol* 44:91–98
- Hoegh-Guldberg O, Mumby PJ, Hooten AJ, Steneck RS, Greenfield P, Gomez E, Harvell CD, Sale PF, Edwards AJ, Caldeira K, Knowlton N, Eakin CM, Iglesias-Prieto R, Muthiga N, Bradbury RH, Dubi A, Hatzilios ME (2007) Coral reefs under rapid climate change and ocean acidification. *Science* 318:1737–1742
- Holcomb M, McCorkle DC, Cohen AL (2010) Long-term effects of nutrient and CO<sub>2</sub> enrichment on the temperate coral *Astrangia*. *J Exp Mar Biol Ecol* 386:27–33
- Houghton JT, Ding Y, Griggs DJ, Noguer M, Van der Linden PJ, Dai X, Maskell K, Johnson CA (2001) Climate change 2001: The scientific basis. Contribution of Working Group I to the Third Assessment Report of the Intergovernmental Panel on Climate Change. Cambridge University Press, Cambridge, p 881
- Hurlbert SH (1984) Pseudoreplication and the design of ecological field experiments. *Ecol Monogr* 54:187–211
- Jury CP, Whitehead RF, Szmant AM (2009) Effects of variations in carbonate chemistry on the calcification rates of *Madracis auretenra* (= *Madracis mirabilis* sensu Wells, 1973): bicarbonate concentrations best predict calcification rates. *Global Change Biol* 16:1632–1644
- Keeling CD (1960) The concentration and isotopic abundances of carbon dioxide in the atmosphere. *Tellus* 12:200–203
- Keeling RF, Piper SC, Bollenbacher AF, Walker JS (2009) Atmospheric CO<sub>2</sub> records from sites in the SIO air sampling network. Trends: A Compendium of Data on Global Change. Carbon Dioxide Information Analysis Center, Oak Ridge National Laboratory, U.S. Department of Energy, Oak Ridge, Tennessee, U.S.A., <http://cdiac.ornl.gov/trends/co2/sio-mlo.html>
- Kleypas JA, Feely RA, Fabry VJ, Langdon C, Sabine CS, Robbins LL (2006) Impacts of ocean acidification on coral reefs and other marine calcifiers: A guide for future research. Report of a Workshop Held 18–20 April 2005, St. Petersburg, FL, sponsored by NSF, NOAA, and the US Geological Survey, p 88
- Langdon C (2000) Review of experimental evidence for effects of CO<sub>2</sub> on calcification of reef-builders. *Proc 9th Int Coral Reef Symp*:1091–1098
- Langdon C, Atkinson MJ (2005) Effect of elevated pCO<sub>2</sub> on photosynthesis and calcification of corals and interactions with seasonal change in temperature/irradiance and nutrient enrichment. *J Geophys Res* 110:C09S07
- Langdon C, Takahashi T, Sweeney C, Chipman D, Goddard J, Marubini F, Aceves H, Barnett H, Atkinson MJ (2000) Effect of calcium carbonate saturation state on the calcification rate of an experimental coral reef. *Global Biogeochem Cycles* 14:639–654
- Lewis E, Wallace DWR (1998) Program developed for CO<sub>2</sub> system calculations. ORNL/CDIAC-105. Carbon Dioxide Information Analysis Center, Oak Ridge National Laboratory. U.S Department of Energy, Oak Ridge, Tennessee
- Luthi D, Le Floch M, Bereiter B, Blunier T, Barnola JM, Siegenthaler U, Raynaud D, Jouzel J, Fischer H, Kawamura K (2008) High-resolution carbon dioxide concentration record 650,000–800,000 years before present. *Nature* 453:379–382
- Maier C, Hegeman J, Weinbauer MG, Gattuso JP (2009) Calcification of the cold-water coral *Lophelia pertusa* under ambient and reduced pH. *Biogeosciences Discussions* 6:1875–1901
- Marubini F, Atkinson MJ (1999) Effects of lowered pH and elevated nitrate on coral calcification. *Mar Ecol Prog Ser* 188:117–121
- Marubini F, Thake B (1999) Bicarbonate addition promotes coral growth. *Limnol Oceanogr* 44:716–720
- Marubini F, Barnett H, Langdon C, Atkinson MJ (2001) Dependence of calcification on light and carbonate ion concentration for the hermatypic coral *Porites compressa*. *Mar Ecol Prog Ser* 220:153–162
- Marubini F, Ferrier-Pages C, Cuif JP (2003) Suppression of skeletal growth in scleractinian corals by decreasing ambient carbonate-ion concentration: a cross-family comparison. *Proc R Soc Lond Ser B* 270:179–184
- Marubini F, Ferrier-Pages C, Furla P, Allemand D (2008) Coral calcification responds to seawater acidification: a working hypothesis towards a physiological mechanism. *Coral Reefs* 27:491–499
- McConnaughey TA, Whelan JF (1997) Calcification generates protons for nutrient and bicarbonate uptake. *Earth Sci Rev* 42:95–117
- Miller MW (1995) Growth of a temperate coral: effects of temperature, light, depth, and heterotrophy. *Mar Ecol Prog Ser* 122:217–225
- Mucci A (1983) The solubility of calcite and aragonite in seawater at various salinities, temperatures, and one atmosphere total pressure. *Am J Sci* 283:780–799
- Neftel A, Moor E, Oeschger H, Stauffer B (1985) Evidence from polar ice cores for the increase in atmospheric CO<sub>2</sub> in the past two centuries. *Nature* 315:45–47
- Piniak GA (2002) Effects of symbiotic status, flow speed, and prey type on prey capture by the facultatively symbiotic temperature coral *Oculina arbuscula*. *Mar Biol* 141:449–455
- Rahmstorf S, Cazenave A, Church JA, Hansen JE, Keeling RF, Parker DE, Somerville RCJ (2007) Recent climate observations compared to projections. *Science* 316:709
- Raven J, Caldeira K, Elderfield H, Hoegh-Guldberg O, Liss P, Riebesell U, Shepherd J, Turley C, Watson A (2005) Ocean acidification due to increasing atmospheric carbon dioxide. The Royal Society, London, p 55
- Reynaud S, Leclercq N, Romaine-Lioud S, Ferrier-Pagés C, Jaubert J, Gattuso JP (2003) Interacting effects of CO<sub>2</sub> partial pressure and temperature on photosynthesis and calcification in a scleractinian coral. *Global Change Biol* 9:1660–1668
- Ries JB, Stanley SM, Hardie LA (2006) Scleractinian corals produce calcite, and grow more slowly, in artificial Cretaceous seawater. *Geology* 34:525–528
- Ries JB, Cohen AL, McCorkle DC (2009) Marine calcifiers exhibit mixed responses to CO<sub>2</sub>-induced ocean acidification. *Geology* 37:1131–1134
- Rodolfo-Metalpa R, Martin S, Ferrier-Pages C, Gattuso JP (2010) Response of the temperate coral *Cladocora caespitosa* to mid- and long-term exposure to pCO<sub>2</sub> and temperature levels projected for the year 2100 AD. *Biogeosci* 7:289–300
- Rogers WH (1993) Regression standard errors in clustered samples. *Stata Tech Bull* 13:19–23
- Roy RN, Roy LN, Vogel KM, Porter-Moore C, Pearson T, Good CE, Millero FJ, Campbell DM (1993) The dissociation constants of carbonic acid in seawater at salinities 5 to 45 and temperatures 0 to 45°C. *Mar Chem* 44:249–267
- Royer DL, Berner RA, Montañez IP, Tabor NJ, Beerling DJ (2004) CO<sub>2</sub> as a primary driver of Phanerozoic climate. *Geol Soc Am Today* 14:4–10
- Ruppert EE, Fox RS (1988) Seashore animals of the Southeast: a guide to common shallow-water invertebrates of the southeastern Atlantic Coast. University of South Carolina Press, Columbia, p 429
- Schneider K, Erez J (2006) The effect of carbonate chemistry on calcification and photosynthesis in the hermatypic coral *Acropora eurystroma*. *Limnol Oceanogr* 51:1284–1293

- Schulz KG, Barcelos e Ramos J, Zeebe RE, Riebesell U (2009) CO<sub>2</sub> perturbation experiments: similarities and differences between dissolved inorganic carbon and total alkalinity manipulations. *Biogeosci* 6:2145–2153
- Scott RW (1995) Global environmental controls on Cretaceous reefal ecosystems. In: Philip J, Skelton PW (eds) *Palaeoenvironmental models for the benthic associations of Cretaceous carbonate platforms in the Tethyan realm*. *Palaeogeogr Palaeoclimatol Palaeoecol* 119: 187–199
- Tyrrell T, Zeebe RE (2004) History of carbonate ion concentration over the last 100 million years. *Geochim Cosmochim Acta* 68:3521–3530